Leaf size determines damage- and herbivore-induced volatile emissions in maize

Jamie M. Waterman[1,2]*, Tristan M. Cofer[1], Ophélie M. Von Laue[1], Pierre Mateo[1], Lei Wang[1], and Matthias Erb[1]*.

[1] Institute of Plant Sciences, University of Bern, Bern, Switzerland

[2] Discipline of Botany, School of Natural Sciences, Trinity College Dublin, Dublin 2, Ireland

* Author(s) for correspondence: watermaj@tcd.ie; matthias.erb@unibe.ch

Author Contributions

JMW conceived the ideas and designed experiments with critical inputs and support from ME. JMW, TMC, OMVL, PM and LW conducted experiments. JMW wrote the first draft of the manuscript and JMW and ME wrote the final version of the manuscript. All authors gave final approval of the manuscript. The authors have no conflicts of interest to declare.

Acknowledgements

We would like to thank Sarah Holder for assistance with plant growth and all members of the Biotic Interactions and Chemical Ecology groups at the University of Bern for helpful discussions. This work was supported by the Swiss National Science Foundation (Grants Nr. 210651 and 200355), the State Secretariat for Education, Research, and Innovation SERI (Project CANWAS), as well as the University of Bern.

Data availability statement

All data will be made available (either as supplemental material or on a data repository) upon publishing the final version, or beforehand upon request.

Abstract:

Stress-induced plant volatiles play an important role in mediating ecological interactions between plants and their environment. The timing and location of the inflicted damage is known to influence the quality and quantity of induced volatile emissions. However, how leaf characteristics and herbivore feeding behavior interact to shape volatile emissions is not well understood. Using a high-throughput volatile profiling system with high temporal resolution, we examined how mechanical damage and herbivore feeding on different leaves shapes plant-level volatile emission patterns in maize. We then tested feeding patterns and resulting consequences on volatile emissions with two generalist herbivores (*Spodoptera exigua* and *Spodoptera littoralis*), and assessed whether feeding preferences are associated with enhanced herbivore performance. We found maize seedlings emit more volatiles when larger leaves are damaged. Larger leaves emitted more volatiles locally, which was the determining factor for higher plant-level emissions. Surprisingly, both *S. exigua* and *S. littoralis* preferentially consumed larger leaves, and thus maximize plant volatile emission without apparent growth benefits. Together, these findings provide an ecophysiological and behavioral mechanism for plant volatile emission patterns, with potentially important implications for volatile-mediated plant-environment interactions.

Introduction

Time and space are important factors that shape plant defense expression and plant-environment interactions (Waterman *et al.*, 2019; Hunziker *et al.*, 2021). It is well known that discrete tissues, especially those with temporally separated development, exhibit specific defense capacities (Köhler *et al.*, 2015; Maag *et al.*, 2015; Maag *et al.*, 2016; Hunziker *et al.*, 2021). In general, evidence suggests that younger plant tissues are typically more well-defended (Ohnmeiss & Baldwin, 2000; Barton *et al.*, 2010). While this is often true for inducible defenses, in some plants, such as maize, older tissues tend to have higher levels of constitutive chemical defenses (Köhler *et al.*, 2015). As such, the specific defense, as well as the nature of its metabolism, are critical considerations. Additionally, spatiotemporal differences in inducible plant defense chemistry often depend on the specific mode of induction. In maize treated with ZmPep3, a peptide associated with regulating responses to wounding, older maize leaves respond more strongly, however, when exposed to herbivore-induced plant volatiles, younger leaves are more responsive (Wang *et al.*, 2023). Even within the same leaf and over relatively short temporal time scales (hours), the timing and position of damage can strongly influence both qualitative and quantitative features of damage-induced responses (Mithöfer *et al.*, 2005; Maag *et al.*, 2016). Tissue-specific patterns may also be temporally dependent. Specifically, in cotton, young leaves from younger plants produced more terpenoids when mechanically damaged in comparison to young leaves in older plants (Eisenring *et al.*, 2017). Similarly, damage to plants at different ontogenetic stages is also an important consideration. In lima bean, tolerance to herbivory through compensatory growth was observed in plants that were previously damaged (primed) during the seedling stages of development and not observed if plants were primed during juvenile and reproductive stages (Bustos-Segura *et al.*, 2022).

An important damage-induced plant defense is the production of damage-induced volatiles. These volatiles are particularly versatile, as they are biosynthesized within tissues, where they can act as a direct defense against biotic stress (Maurya *et al.*, 2020; Chen *et al.*, 2021; Chen *et al.*, 2023). These volatiles are also emitted into the environment, where they have broad ecological relevance (Escobar-Bravo *et al.*, 2023). Plant-derived volatiles can serve as within-plant signaling molecules (Heil & Silva Bueno, 2007), attract herbivore natural enemies (Schnee *et al.*, 2006; Turlings & Erb, 2018), influence herbivore oviposition (Hajdu *et al.*, 2024), mediate plant-pollinator interactions (Groen *et al.*, 2016) and mediate plant-plant interactions (Wang *et al.*, 2023; Waterman *et al.*, 2024).

Damage-induced volatiles can be manipulated by herbivores, which employ several strategies to reduce plant volatile emissions, potentially minimizing detection from natural enemies such as predators and parasitoids. For example, the saliva of the caterpillar *Helicoverpa zea*, which can be secreted onto plant tissues during feeding, contains the enzyme glucose oxidase, which causes stomatal closure and reduced the emission of some volatiles (Lin *et al.*, 2021). Conversely, herbivores can also betray themselves by attracting natural enemies, for example *Manduca sexta* oral secretions decrease the *(Z)*/*(E)* ratio of green leaf volatiles emitted by plants during feeding, which increases herbivore attractiveness to predators (Allmann & Baldwin, 2010). While herbivore feeding patterns can influence plant phenotypes, within-plant spatiotemporal phenotypic variation can also influence herbivore feeding behavior, and in turn shape wider plant-environment interactions (Bellec *et al.*, 2022; Orrock *et al.*, 2022). While plant traits have been shown to influence herbivore behavior, broadly applicable patterns are difficult to identify and many herbivore-feeding patterns may be explained by processes and environmental features independent of the plant (The Herbivory Variability Network* † *et al.*, 2023; Pan & Wetzel, 2024). Importantly, the degree

to which herbivore feeding patterns and preferences align with inherent spatiotemporal differences in volatile induction is unclear.

The aim of our study was to test how damage done to different leaves affects the emission of ecologically relevant induced plant volatiles at the plant level, and to identify the mechanistic basis for these differences. Further, to better understand the potential implications of these differences, we investigated the feeding patterns of two lepidopteran herbivores, and the resulting impact on herbivore-induced volatile emissions. We tested a number of biochemical, chemical and morphological leaf traits across developmental stages, and manipulated leaf size to build a mechanistic understanding of what drives differences in emission between leaves. Additionally, we determined that herbivores preferentially fed on larger leaves without any apparent performance benefit, and thus maximized plant volatile emissions. Together, these findings reveal leaf size as an important determinant of plant-level volatile emissions and demonstrate that two generalist herbivores feed in a way that maximizes rather than minimizes leaf volatile emissions, without apparent direct benefits.

Materials and Methods

Plant and insect growth

V2- and V3-stage maize seedlings (*Zea mays*, B73) were used throughout this study. At the V2 stage, maize has four leaves: two are fully developed, one is expanding and one is emerging. At the V3 stage maize has 5 leaves: three are fully developed, one is expanding and one is emerging. At these growth stages, maize plants are often attacked by herbivores such as *Spodoptera* spp. (van den Berg *et al.*, 2021). Maize plants were grown in commercial potting soil (Selmaterra, BiglerSamen, Switzerland) in 180 ml pots. Plants were grown in

124 greenhouse conditions and supplemented with artificial lights (*ca*. 300 µmol m^{-2} s^{-1}). The
125 greenhouse was kept at 22 ± 2 °C, 40–60% relative humidity, with a 14 h : 10 h, light : dark
126 cycle. *Spodoptera exigua* (Frontier Agricultural Sciences, USA) and *Spodoptera littoralis*
127 (University of Neuchatel, Switzerland) were reared from eggs on artificial diet (Maag *et al.*,
128 2014) and used for experiments when they reached the 4th instar stage. All experiments were
129 conducted between the hours of 10:00 and 20:00 under full-light conditions.

130

131 Plant damage

132 To mimic dynamic patterns, we damaged plants three times in *ca.* 30 min intervals. Each
133 damage event consisted of two hemostat wounds, one on each side of the midvein. The first
134 damage event was at the base of the leaf, the second in the middle, and the third at the tip.
135 The extent and relative spacing of damage was identical across leaves, so that for each leaf
136 the tip, middle and base of each leaf was damaged. Damage was either inflicted on leaves of
137 intact plants or detached leaves as specified in the text and figure legends.

138

139 Detached leaf assay

140 Leaves were dissected following the protocol of Wang et al., 2023. In brief, leaves were cut at
141 the base from maize seedlings while submerged in milliQ water. The cut base of leaves
142 remained submerged in water for 2 hr to allow for tissues to recover from dissections, prior to
143 damage treatments. Volatile emissions from individual leaves were measured the same way as
144 intact seedlings.

145

146 Volatile sampling

147 Entire seedlings or detached leaves were placed in transparent glass chambers (Ø×H 12 × 45
148 cm) that were sealed other than an clean airflow inlet and an outlet. Clean air was supplied at
149 a flow-rate of 0.8 L min^{-1}. Volatiles were measured with a high-throughput platform
150 comprised of a proton transfer reaction time-of-flight mass spectrometer (PTR-ToF-MS;
151 Tofwerk, Switzerland) and a custom-made automated headspace sampling system (Gonin *et*
152 *al.*, 2018). The outlet of the chamber was accessible to the autosampler/PTR-ToF-MS system.
153 The PTR-ToF-MS system drew air at 0.1 L min^{-1}. Between samples, a zero-gas measurement
154 was performed for 3 s to flush the system. At each time point, volatiles were continuously
155 measured for 25-30 s and averaged to a single mean per sample. Complete mass spectra (0-
156 500 m/z) were recorded in positive mode at *ca.* 10 Hz. The PTR was operated at 100 ˚C and
157 an E/N of approximately 120 Td. The volatile data extraction and processing were conducted
158 using Tofware software package v3.2.2 (Tofwerk, Switzerland). Protonated compounds were
159 identified based on their molecular weight + 1. During volatile collection, LED lights
160 (DYNA, heliospectra) were placed *ca.* 80 cm above the glass cylinders and provided light at
161 300 µmol m^{-2} s^{-1}. Identical light : dark cycle timing as in the greenhouse for plant growth
162 was used. To calculate 'total' volatile emissions, we took the integral of the emission curve
163 over time, in other words, the sum of each individual volatile measurement time point over
164 the experimental period.

165

166 <u>Gene expression</u>

167 1.5 hr after the first leaf damage, each leaf (leaf 2, 3 and 4) was harvested and flash frozen on
168 liquid nitrogen. Total RNA extraction and purification, genomic DNA removal, cDNA
169 synthesis and quantification of gene expression were conducted identically to Waterman et
170 al., 2024. Quantitative reverse transcription polymerase chain reaction (qRT-PCR) was

171 performed using ORA SEE qPCR Mix (highQu GmbH, Germany) on an Applied Biosystems
172 QuantStudio 5 Real-Time PCR system. The normalized expression (NE) values were
173 calculated as in Waterman et al., 2024 using ubiquitin (UBI1) as the reference gene. Gene
174 identifiers and primer sequences are listed in Supplementary Table 1.

175

176 HDMBOA-Glc quantification

177 Approximately 100 mg of fresh frozen, finely ground leaf was extracted in 1 mL acidified
178 MeOH/H_2O 70:30 v/v spiked with 0.1% formic acid. Extracts were vortexed for 10 seconds
179 and centrifuged at 13000 rpm for 20 min at 10 °C. The supernatant was removed and used for
180 subsequent quantification. HDMBOA-Glc profiling was performed with an Acquity i-Class
181 UPLC system equipped with a photodiode array detector (PDA) and a single quadrupole
182 detector (QDa) with electrospray source (Waters, USA). Gradient elution was performed on
183 an Acquity BEH C18 column (1.7 µm, 2.1 × 100 mm, Waters, USA).The elution conditions
184 were as follows: 90-70% A over 3 min, 70-60% A over 1 min, 40-100% B over 1 min,
185 holding at 100% B for 2.5 min, holding at 90% A for 1.5 min where A = 0.1% formic
186 acid/water and B = 0.1% formic acid/acetonitrile. The flow rate was 0.4 mL/min. The
187 temperature of the column was maintained at 40 °C, and the injection volume was 1 µL.
188 Absolute quantities were determined using standard curves of the corresponding pure
189 HDMBOA-Glc.

190

191 Stomatal density

192 Clear nail polish was painted onto either the base, middle or tip of the abaxial and adaxial
193 side of each leaf. Once hardened, the polish was removed with double-sided sticky tape,
194 creating an epidermal imprint. Imprints were mounted onto glass microscope slides and

imaged with a Leica DM2500 optical microscope coupled to an HD digital microscope camera (Leica MC170 HD) (Leica Microsystems, Germany). The density of stomata on each imprint was calculated based on the average of three distinct and non-overlapping fields of view.

Herbivore feeding on intact plants

To assess damage patterns on intact V2-stage maize seedlings, a single *S. exigua* or *S. littoralis* larva was placed on either leaf 2 or leaf 3. Herbivores were allowed to feed for 6 hr. At the end of the feeding period, damaged area of each leaf was estimated visually. To convert this estimated value on a per-leaf basis into the percentage of total plant damage, a subset of plants was kept undamaged. Using ImageJ (National Institutes of Health, USA), the average surface area of each leaf on these control plants was used as a reference, and the percent area contributed by each individual leaf to the total surface area of the plant was calculated. In other words, the estimated percentage of a given leaf removed by herbivores was multiplied the percentage of the total area of all leaves made up by said leaf.

Herbivore feeding and performance on individual leaves

To assess herbivore feeding on detached leaf 2 and leaf 3, leaves were dissected as previously described (see *detached leaf assay*). One 4th instar larva was placed at the base of each leaf and allowed to feed for 6 hr. The area of tissue damage was calculated using ImageJ and methods described in (Waterman *et al.*, 2021). To calculate the biomass of tissue consumed we multiplied the area of damage by the leaf mass per area (LMA), which is descried as the ratio of mass per unit area (KATTGE *et al.*, 2011). This was calculated for leaf 2 (LMA = 0.0031, $n = 6$) and leaf 3 (LMA = 0.0025, $n = 6$). To assess the relative growth rate of

219 herbivores on detached leaves, larvae were placed on leaves in an identical fashion to
220 described above, however were allowed to feed for 48 hr, with leaves being replaced at the 24
221 hr mark to prevent desiccation. Relative growth rate was calculated as: ((final larval weight –
222 initial larval weight) / initial larval weight) / # of days of feeding, as previously described
223 (Waterman *et al.*, 2021).

224

225 Statistical analyses

226 All statistical analyses were conducted in R version 4.2.2 (R Core Team, 2022). Gene
227 expression and stomatal density were analyzed using two-way ANOVA (Type = II). Gene
228 expression was analyzed on log-transformed normalized expression values. HDMBOA-Glc
229 was analyzed with one-way ANOVA within each leaf for plants where leaf 2 and leaf 3 were
230 damaged. As data from plants with leaf 4 damage did not meet the assumptions of ANOVA,
231 differences in HDMBOA-Glc between leaves of these plants were determined using a
232 Kruskal-Wallis test. Differences in detached leaf biomass were also analyzed with one-way
233 ANOVA. Where necessary, to obtain heteroscedasticity-consistent standard errors, White-
234 adjusted ANOVAs were used (White, 1980). To determine leaf damage area by herbivores in
235 intact seedlings, as the assumptions of ANOVA were not met, Kruskal Wallis tests were used.
236 For herbivore feeding and performance assays in detached leaves, Welch's two-sample t-tests
237 were used to compare leaf 2 and leaf 3. Statistical test summaries are included as
238 supplemental information (Supplemental Tables 2 and 3).

239

240 **Results**

241 ***Plant-level volatile emissions are determined by damage position***

In order to determine how damage position impacts induced plant-level volatile emissions, we damaged each leaf of a V2-stage maize seedling individually (Fig 1A) and measured induced volatile emissions. Green leaf volatile emissions, which are strongly localized to wound sites (Matsui, 2006), were comparable across treatments, with the exception of plants where the youngest leaf (leaf 4) was damaged, which resulted in, generally, lower green leaf volatile emissions (Fig 1B). Plant-level emissions of terpenes and indole were strongly influenced by damage location. Plants damaged on leaf 3 had the highest emission levels of monoterpenes [$C_{10}H_{17}^{+}$, m/z = 137.13], sesquiterpenes [$C_{15}H_{25}^{+}$, m/z = 205.20], and 4,8,12-trimethyltrideca-1,3,7,11-tetraene (TMTT) [$C_{16}H_{27}^{+}$, m/z = 219.21], 4,8-dimethylnona-1,3,7-triene (DMNT) [$C_{11}H_{19}^{+}$, m/z = 151.15] and indole [$C_8H_8N^{+}$, m/z = 118.07], followed by leaf 2 and leaf 4 (Fig 1C). Thus, which leaf is damaged is a strong determinant of plant-level volatile emissions.

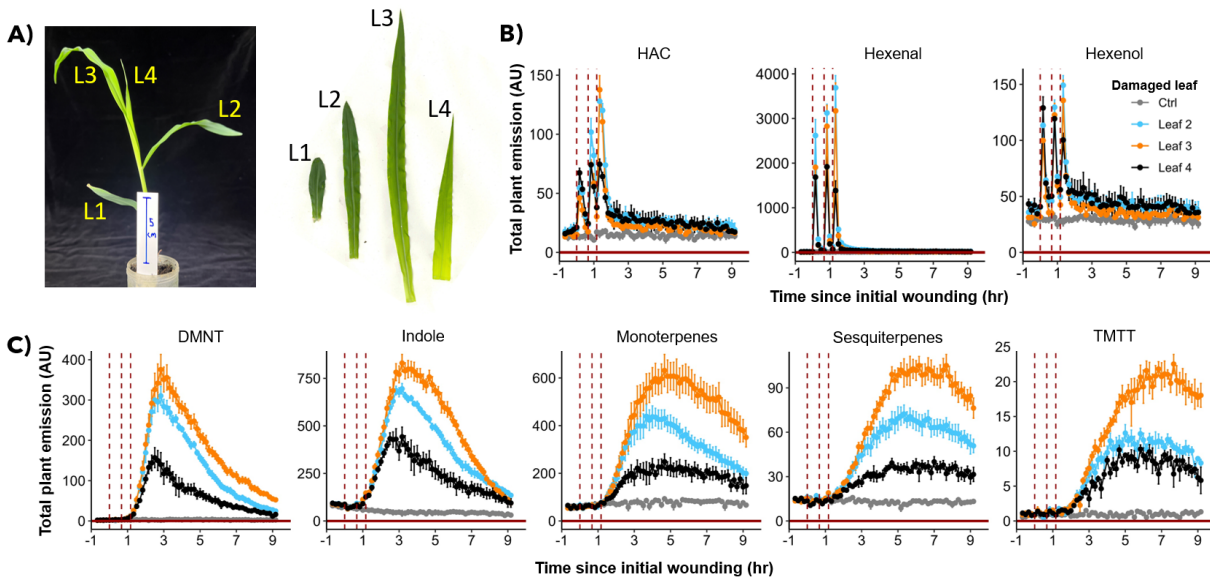

Figure 1. Plant-level volatile emissions depends on which leaves are damaged. A) The different leaves and respective sizes of intact V2-stage maize seedlings. Emission kinetics of B) green leaf volatiles and C) terpenes and indole are shown. Perforated vertical lines depict the timing of each mechanical damage entry. Abbreviations: HAC, Hexenyl acetate; DMNT, 4,8-dimethylnona-1,3,7-triene; TMTT, 4,8,12-trimethyltrideca-1,3,7,11-tetraene. Compounds were identified based on their molecular weight + 1, as all compounds were protonated. HAC: m/z = 143.11, Hexenal: m/z = 99.08, Hexenol: m/z = 101.0, DMNT: m/z = 151.15, Indole: m/z = 118.07, Monoterpenes: m/z = 137.13, Sesquiterpenes: m/z = 205.20, TMTT: m/z = 219.21. Colored points = mean ± SE. *n* = 5.

255

256 ***Minimal differences in local damage inducibility of volatile biosynthesis genes and direct***
257 ***defenses***

258 To test whether damage to the different leaves leads to differential local and systemic defense
259 induction, which may determine leaf- and plant-level volatile emissions, we measured
260 terpene and indole biosynthesis gene expression. Terpene synthase 2 and 10 (TPS2 and
261 TPS10), as well as dimethylnonatriene/trimethyletetradecatetraene synthase (CYP92C5) are
262 rate limiting for terpene production, and indole-3-glycerol phosphate lyase (IGL) is rate
263 limiting for volatile indole biosynthesis (Frey *et al.*, 2000; Richter *et al.*, 2016; Block *et al.*,
264 2019). We also measured HDMBOA-Glc levels as a major marker of non-volatile defense
265 induction in maize to test whether spatial defense patterns may be generalizable (Li *et al.*,
266 2018). Following damage to individual leaves, all tested genes were significantly induced
267 both locally and systemically (Fig 2). Local induction was generally highest in leaf 2 and leaf
268 3 and lower in leaf 4 (Fig 2). Systemic induction was similar across treatments. HDMBOA-
269 Glc was induced locally, but not systemically across all leaves at comparable concentrations,
270 although the effect was only significant for leaf 2 and leaf 3 (Supplemental Fig 1). Thus, the
271 differences in plant volatile emissions upon damage of cannot be explained by differential
272 local and systemic inducibility.

273

274

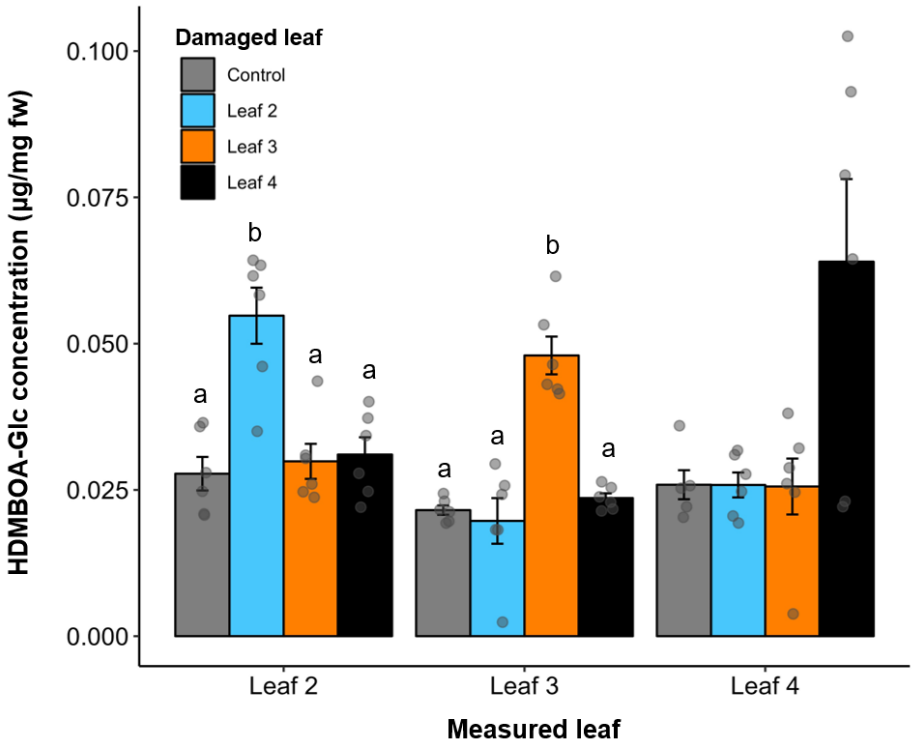

Supplemental Figure 1. HDMBOA-Glc is similarly induced across leaves in intact V2-stage maize seedlings. Lowercase letters indicate significant differences between damage sites within a given leaf based on multiple comparisons tests. Grey points represent biological replicates. Bars = mean ± SE. *n* = 5-6.

285

286

287

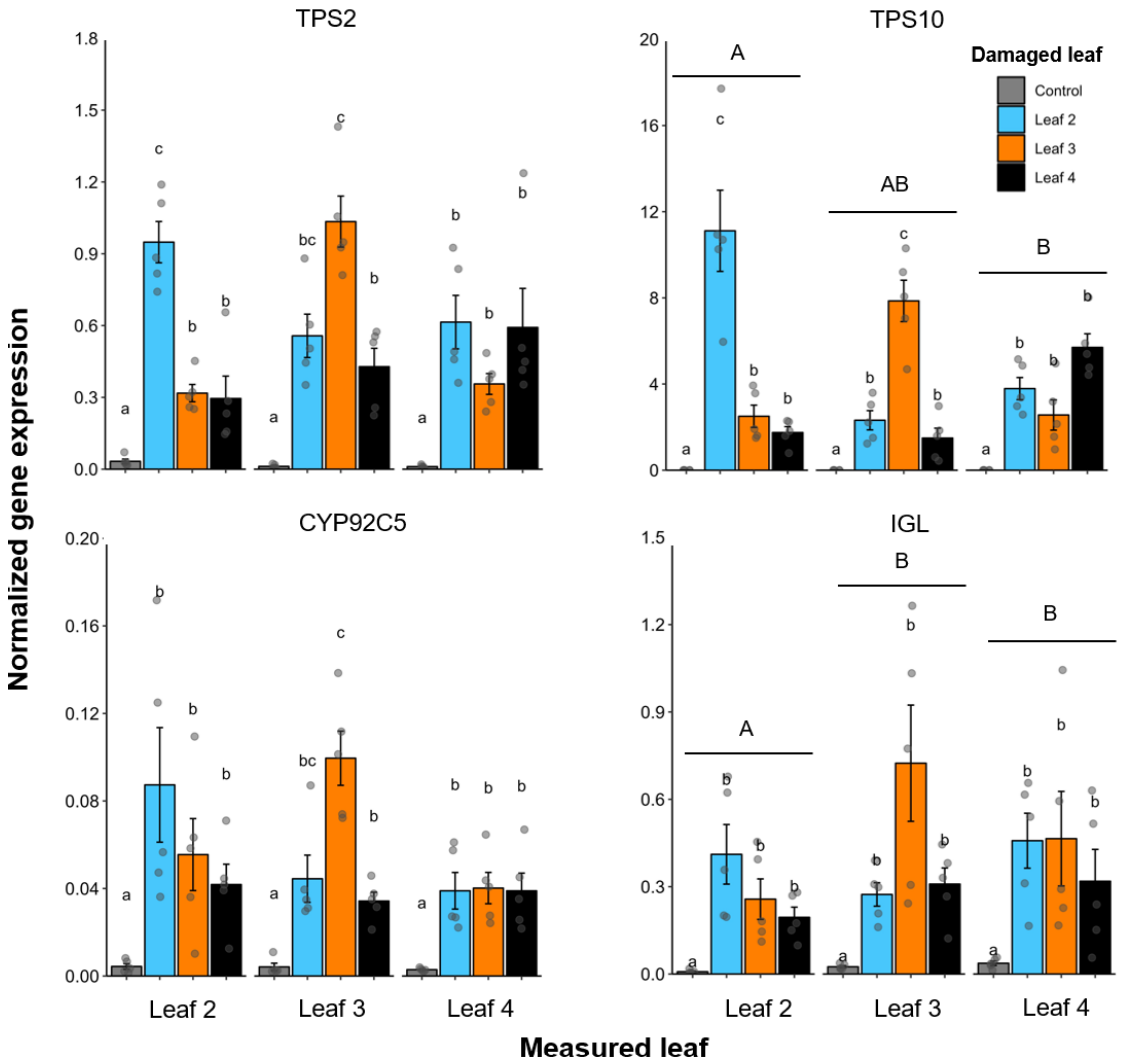

Figure 2. Minimal differences in volatile biosynthesis inducibility of different leaves in intact plants. Expression of terpene and indole biosynthesis genes are shown. Abbreviations: TPS2, terpene synthase 2; TPS10, terpene synthase 10; CYP92C5, Dimethylnonatriene/trimethyltetradecatetraene synthase, IGL, indole-3-glycerol phosphate lyase. Lowercase letters indicate significant differences between damage sites within a given leaf and uppercase letters indicate overall differences between leaves, regardless of which left was damaged (based on multiple comparisons tests). Grey points represent biological replicates. Bars = mean ± SE. $n = 5$.

Plant volatile emissions strongly correlate with the size of the damaged leaf

One apparent difference between the leaves is their size, both in terms of biomass and surface area (Fig 1A). Thus, we hypothesized that larger leaves may result in higher volatile release upon damage. We used biomass as the principal metric of size, which is also highly correlated with leaf surface area across all leaves, and this correlation is maintained across

developmental stages (Supplemental Fig 2). We found strong and significant correlations between the biomass of the damaged leaf and plant-level volatile emissions (Fig 3A). We also found similar correlations for leaf-level emissions in individual detached damaged leaves of V2- and V3-stage seedlings (Fig 3B; Supplemental Fig 3). There was also a significant linear relationship between volatile emissions and the surface area of the damaged leaf in both seedling stages (albeit slightly weaker than the relationship with damaged leaf mass; Supplemental Fig 4). Immature leaves (leaf 3 and 4 for V2-stage seedlings and leaf 4 and 5 for V3-stage seedlings) showed the strongest relationship between emission and size across the different leaves (Fig 3; Supplemental Fig 4). Interestingly, leaf 2 consistently showed higher volatile emissions than expected for its size in V2-stage seedlings, as did leaf 3 in V3-stage seedlings (Fig 3).

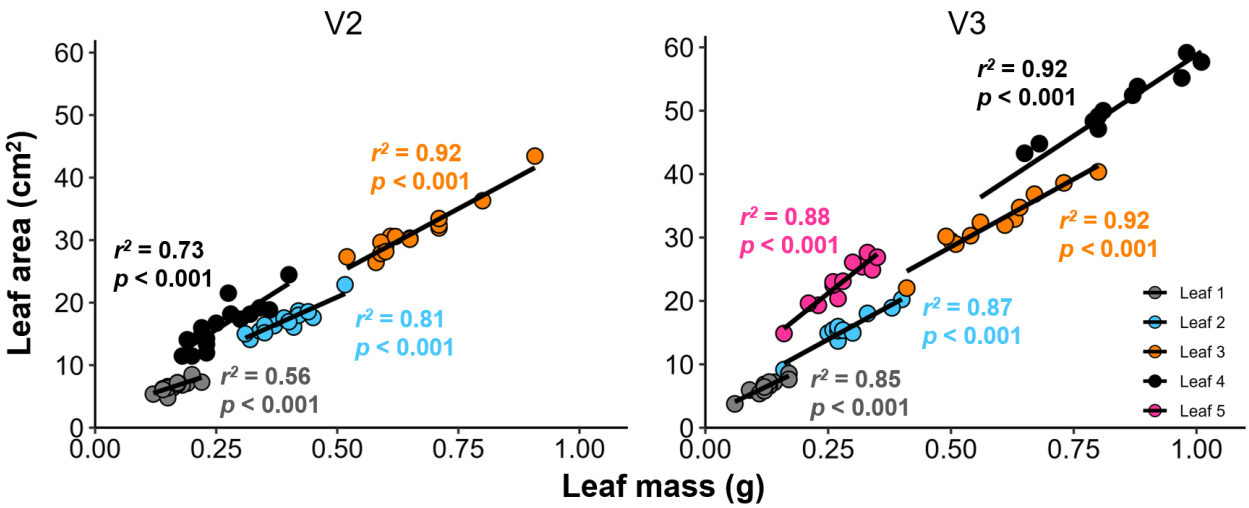

Supplemental Figure 2. Strong positive relationship between leaf mass and leaf area in both V2-stage and V3-stage maize seedlings. Black lines represent linear regression for significant linear relationships for each leaf. Colored points depict biological replicates of different leaves. Plants used were undamaged. n = 12-16.

308

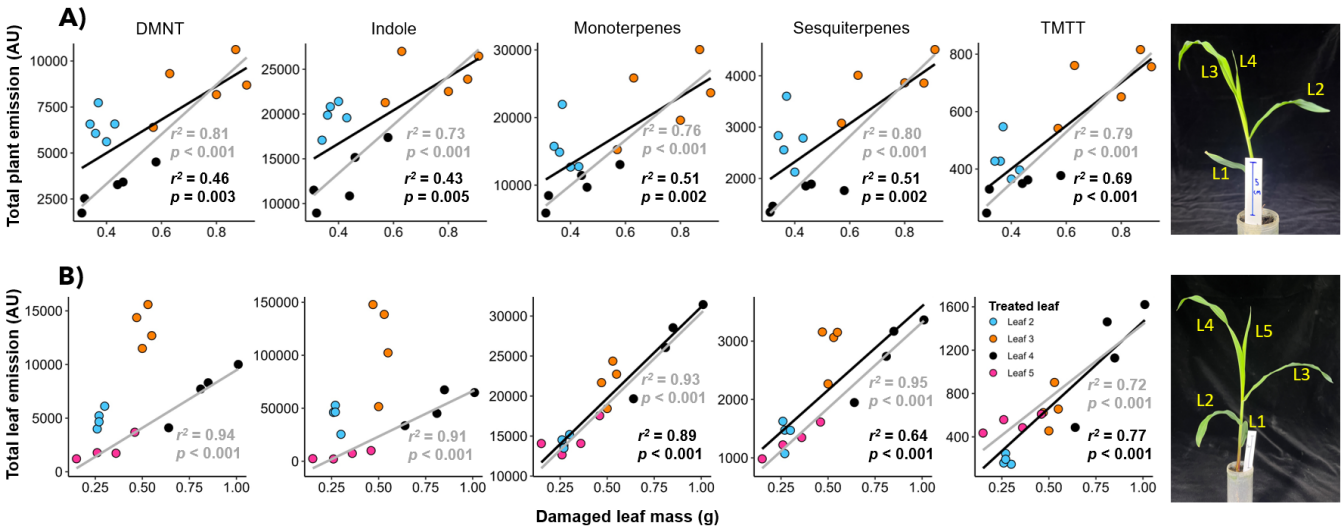

Figure 3. Whole-plant- and leaf-level volatile emissions strongly correlate with the mass of the damaged leaf. Colored points represent biological replicates and depict the relationship between total volatile emission (sum of individual measurement time points over 9 hr; see Materials and Methods, *Volatile sampling*) and leaf biomass in A) intact V2-stage seedlings and B) detached leaves of V3-stage seedlings. Black lines represent linear regression for significant linear relationships between all leaves. Grey lines represent linear regression for significant linear relationships between immature leaves (leaf 3 and leaf 4 for V2-stage; leaf 4 and leaf 5 for V3-stage). Abbreviations: DMNT, 4,8-dimethylnona-1,3,7-triene; TMTT, 4,8,12-trimethyltrideca-1,3,7,11-tetraene. Compounds were identified based on their molecular weight + 1, as all compounds were protonated. DMNT: m/z = 151.15, Indole: m/z = 118.07, Monoterpenes: m/z = 137.13, Sesquiterpenes: m/z = 205.20, TMTT: m/z = 219.21. n = 5 for V2-stage seedlings, n = 4 for V3-stage leaves.

309

310

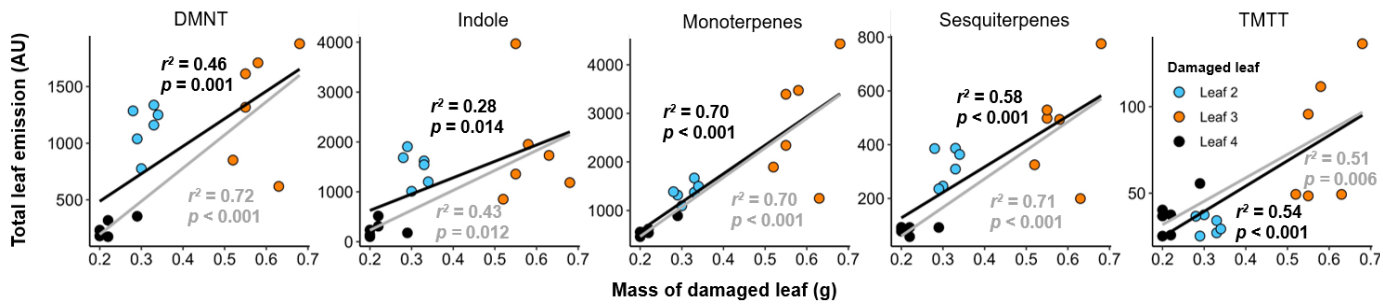

Supplemental Figure 3. Detached maize leaves from V2-stage seedlings maintain the same emission-leaf size relationships as when leaves of intact plants are damaged. Colored points represent biological replicates and depict the relationship between total volatile emission (sum of individual measurement time points over 9 hr; see Materials and Methods, *Volatile sampling*) and leaf biomass. Black lines represent linear regression for significant correlations between all leaves. Grey lines represent linear regression for significant linear relationships between immature leaves (leaf 3 and leaf 4). Abbreviations: DMNT, 4,8-dimethylnona-1,3,7-triene; TMTT, 4,8,12-trimethyltrideca-1,3,7,11-tetraene. Compounds were identified based on their molecular weight + 1, as all compounds were protonated. DMNT: m/z = 151.15, Indole: m/z = 118.07, Monoterpenes: m/z = 137.13, Sesquiterpenes: m/z = 205.20, TMTT: m/z = 219.21. Error bars = SE. n = 6.

311

312

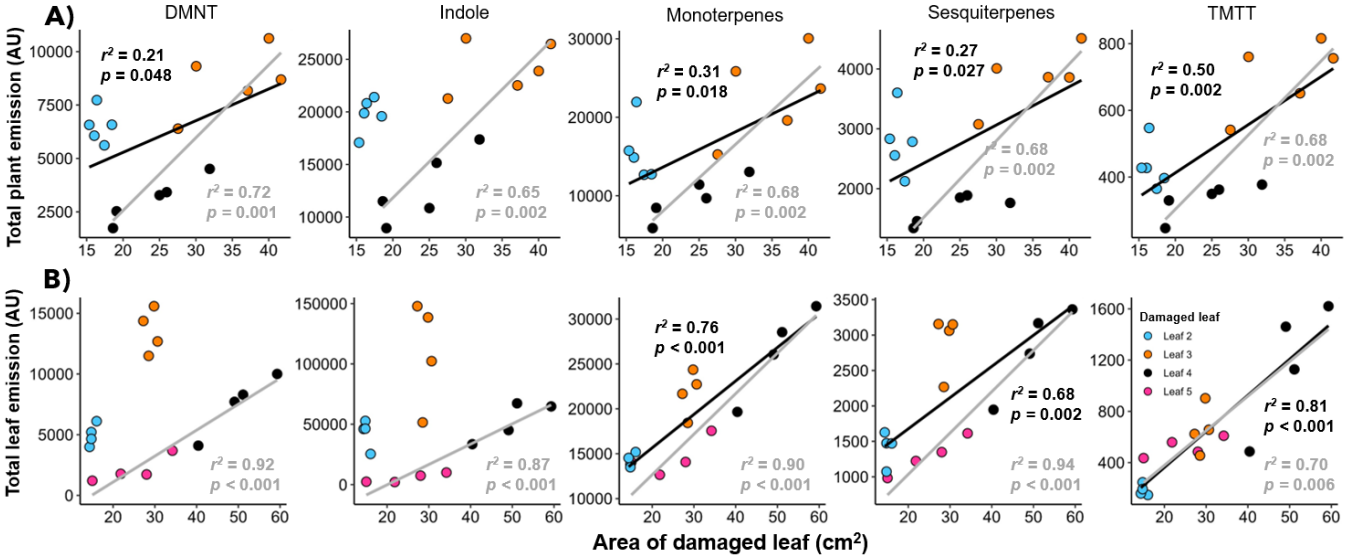

Supplemental Figure 4. Relationships are maintained between volatile emissions and the area of damaged leaves across developmental stages. Colored points represent biological replicates and depict the relationship between total emission (sum of individual measurement time points over 9 hr; see Materials and Methods, *Volatile sampling*) of plant volatiles and leaf surface area in A) intact V2-stage seedlings and B) detached leaves of V3-stage seedlings. Black lines represent linear regression for significant correlations between all leaves. Grey lines represent linear regression for significant linear relationships between immature leaves (leaf 3 and leaf 4 for V2-stage; leaf 4 and leaf 5 for V3-stage). Abbreviations: DMNT, 4,8-dimethylnona-1,3,7-triene; TMTT, 4,8,12-trimethyltrideca-1,3,7,11-tetraene. Compounds were identified based on their molecular weight + 1, as all compounds were protonated. DMNT: m/z = 151.15, Indole: m/z = 118.07, Monoterpenes: m/z = 137.13, Sesquiterpenes: m/z = 205.20, TMTT: m/z = 219.21. Error bars = SE. n = 5 for V2-stage seedlings, n = 4 for V3-stage leaves.

313

314

315 ***Standardizing leaf area results in similar induced volatile emissions***

316 In order to investigate whether leaf size is the driving factor for induced volatile emission,
317 we compared entire detached leaves with leaves that were all cut to the biomass of leaf 4 (Fig
318 4A-C). Entire detached leaves showed similar emission kinetics to entire plants, where leaf 3
319 emitted the most volatiles (Fig 4D). When cut to equal size, emissions of damage-induced
320 volatiles were similar between leaf 2 and 3 (Fig 4E). For all compounds except TMTT, both
321 leaf 2 and leaf 3 emitted more volatiles than leaf 4 when cut to equal biomass. As terpene and
322 indole emission are controlled by stomata, we measured stomatal densities between leaf 2 and

leaf 3 and found no differences (Supplemental Fig 5). Maize leaf-development occurs on a gradient from the tip to base, with the tip being most developed and the base being least developed (Raissig *et al.*, 2017; Wang *et al.*, 2019). Accordingly, the base of leaves has fewer developed stomata than the other sections (Supplemental Fig 5). When cutting leaves to similar sizes, we only removed the bottom portion (with fewer on stomata for both leaves). There were no differences stomatal density between the middle and tip in leaves 2 and 3, and no differences in stomatal density were observed between leaf 2 and leaf 3 (Supplemental Fig 4), thus ruling out stomatal density as a driver of differential volatile emissions between these two leaves.

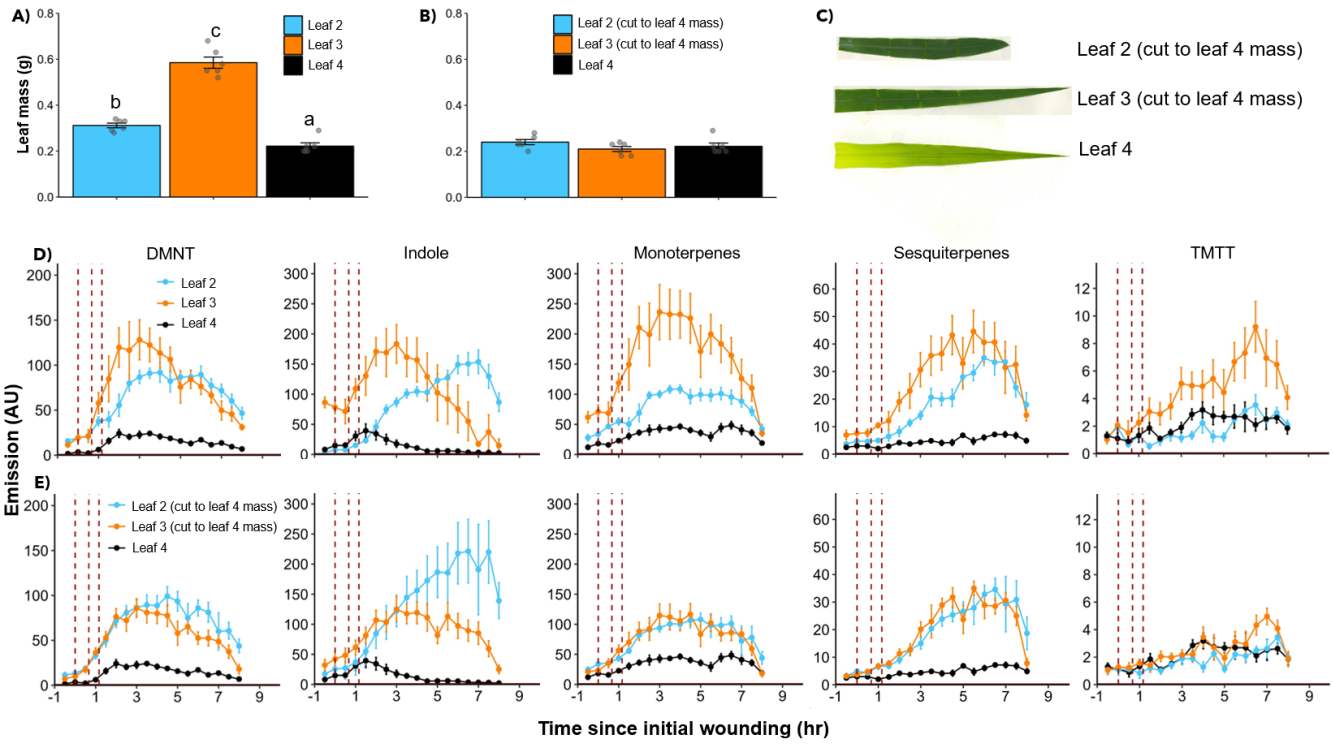

Figure 4. Standardizing leaf biomass results in similar induced volatile emissions between detached leaves of V2-stage seedlings. Biomass of A) entire detached leaves of V2-stage seedlings and B) V2-stage leaves 2 and 3 cut to the biomass of Leaf 4. C) V2-stage leaves 2-4 when standardized to size. Emission kinetics of D) entire detached V2-stage leaves and E) V2-stage leaves cut to leaf 4 biomass. Perforated vertical lines depict the timing of each mechanical damage entry. Lowercase letters indicate significant differences between leaves based on multiple comparisons tests. Abbreviations: DMNT, 4,8-dimethylnona-1,3,7-triene; TMTT, 4,8,12-trimethyltrideca-1,3,7,11-tetraene. Compounds were identified based on their molecular weight + 1, as all compounds were protonated. DMNT: m/z = 151.15, Indole: m/z = 118.07, Monoterpenes: m/z = 137.13, Sesquiterpenes: m/z = 205.20, TMTT: m/z = 219.21. Grey points represent biological replicates. Bars = mean ± SE. n = 6.

333

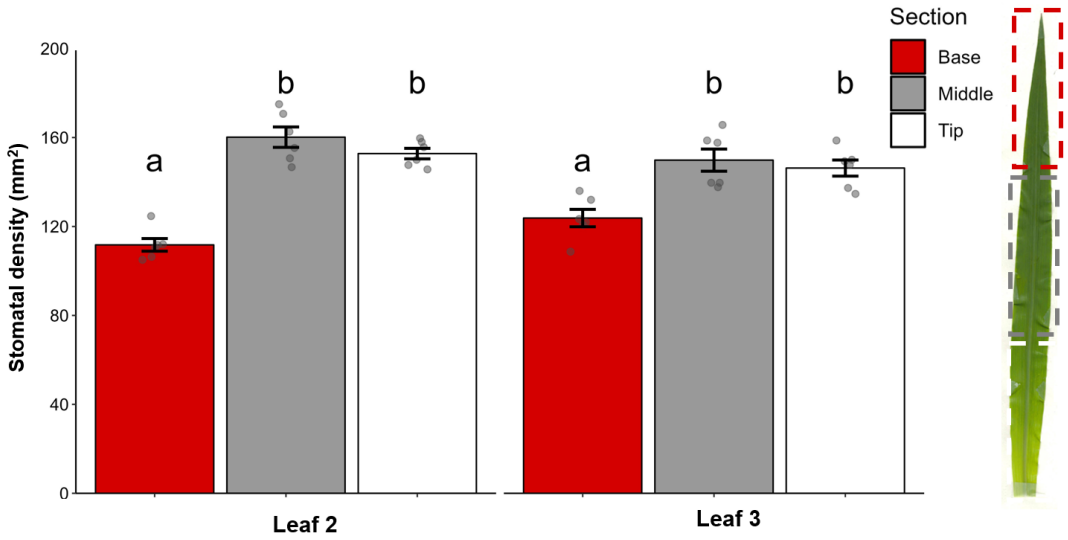

Supplemental Figure 4. Stomatal patterns are similar between leaf 2 and leaf 3 in V2-stage maize seedlings. Stomatal density (abaxial and adaxial sides combined) of the sections of leaf 2 and leaf 3. Differing lowercase letters indicate significant differences between leaf and location on leaf based on multiple comparisons tests. Grey points represent biological replicates. Bars = mean ± SE. n = 6.

334

335

336 ***Generalist herbivores prefer to feed on leaves with higher volatile inducibility***

337 To test how herbivore feeding interacts with spatiotemporal differences in volatile emission,
338 we placed a single *Spodoptera exigua* or *Spodoptera littoralis* larva on either leaf 2 or leaf 3
339 of V2-stage maize seedlings and tracked their feeding patterns. For *S. exigua*, we found that,
340 regardless of starting position, herbivores consistently eat mostly leaf 3 (Fig 5). When placed
341 on leaf 3, only 6.3% of larvae fed on leaf 2 and 84.4% fed on leaf 3 (Table 1). Even when
342 placed on leaf 2, only 40.6% of larvae fed on leaf 2 and 81.3% of larvae fed on leaf 3. When
343 herbivores were placed on leaf 2, damage area on leaf 4 was similar to leaf 2, and when
344 placed on leaf 3, leaf 4 showed comparable damage levels to leaf 3. The trends for *S.*
345 *littoralis* were similar to *S. exigua* with some key differences. Firstly, all *S. exigua* larvae
346 placed on plants fed (N = 64). For *S. littoralis* only 36/64 fed (56%). *S. littoralis* also

347 appeared far more mobile; many dropped off of into the soil at the base of the plant and did
348 not eat. For *S. littoralis* larvae placed on leaf 2, although trends matched *S.exigua* patterns,
349 differences in feeding area between leaves were not significant (Fig 5). In addition to damage
350 area, for leaf 2-placed *S. littoralis*, the number of larvae feeding on each leaf was similar
351 between leaves, whereas this was not the case for *S. exigua* placed on leaf 2 (Table 1).
352 However, for larvae placed on leaf 3, the *S. littoralis* patterns matched those of *S. exigua*,
353 whereby leaf 3 and leaf 4 had significantly more damage than the other leaves (Fig 5). Thus
354 indicating that generalist herbivores preferentially feed on the leaves that result in the greatest
355 plant-level damaged-induced volatile emissions.

356

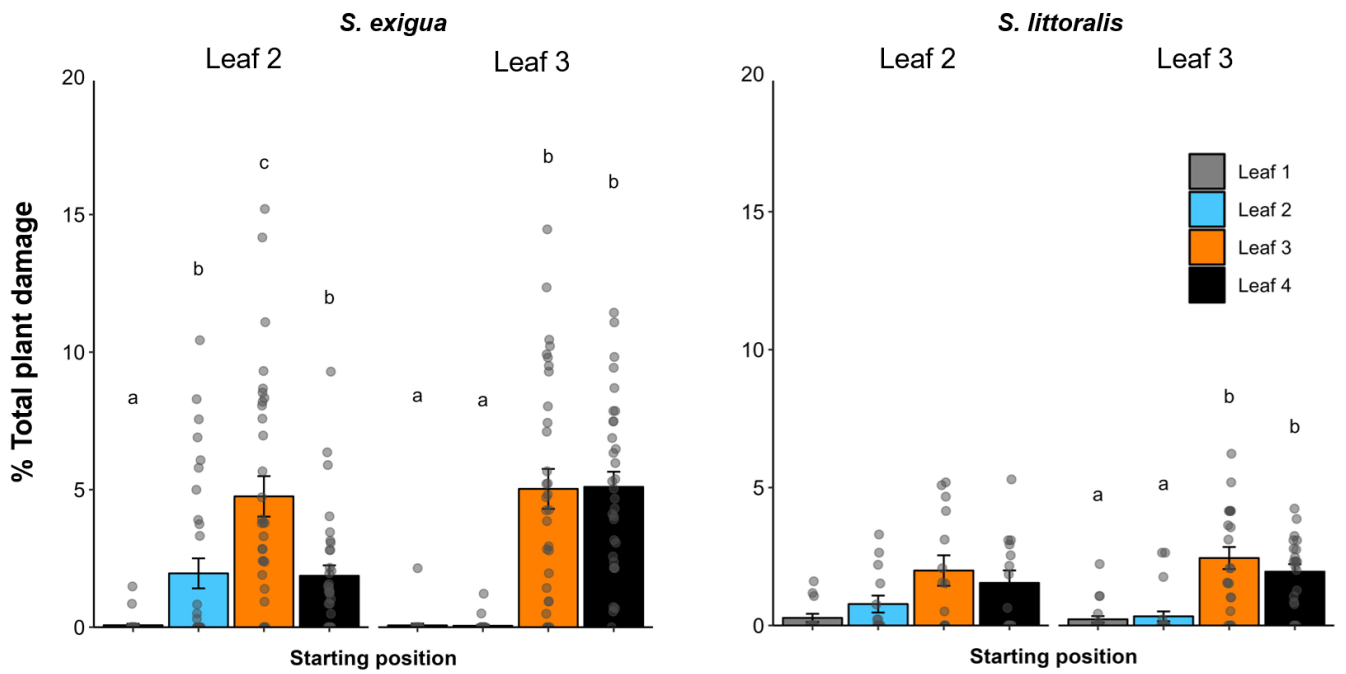

Figure 5. Generalist herbivores consistently feed heavily on leaf 3 regardless of starting position. The percentages of total plant damage (on V2-stage seedlings) done on each leaf for both *Spodoptera exigua* and *S. littoralis*. Larvae were either placed on leaf 2 or leaf 3 (starting position). For each herbivore species, lowercase letters indicate significant differences between leaves within a given herbivore starting position based on pairwise Wilcox tests. Grey points represent biological replicates. Bars = mean ± SE. For *S. exigua*, n = 32 and for *S. littoralis*, n = 14-22.

357

358

359

Table 1. Intact maize seedling herbivore feeding information table.

Starting position	Leaf	# of larvae feeding (total)	% of larvae feeding
Spodoptera exigua			
L2			
	1	2 (32)	6.3 %
	2	13 (32)	40.6 %
	3	26 (32)	81.3 %
	4	23 (32)	71.9 %
L3			
	1	1 (32)	3.1 %
	2	2 (32)	6.3 %
	3	27 (32)	84.4 %
	4	31 (32)	96.9 %
Spodoptera littoralis			
L2			
	1	3 (14)	21.5%
	2	7 (14)	50 %
	3	9 (14)	64.3 %
	4	8 (14)	57.1 %
L3			
	1	5 (22)	22.7 %
	2	4 (22)	18.2 %
	3	18 (22)	81.8 %
	4	18 (22)	81.8 %

360

361

362 Similar to mechanical damage patterns, we found that, under authentic herbivory conditions,
363 leaf 3 emitted higher amounts of all measured volatiles compared to leaf 2 in detached leaves
364 (Fig 6A). In intact seedlings, total emissions from *S. exigua*-infested plants were positively
365 correlated with leaf 3 damage for all measured compounds (Fig 6B): This was not the case
366 for leaf 2, where no positive correlations were observed, and TMTT emission even showed a
367 significant negative relationship with leaf 2 damage (Fig 6C). Thus confirming that, like

368 mechanical damage, herbivory on leaf 3 is of the greatest consequence to total volatile

369 emissions in maize seedlings.

370

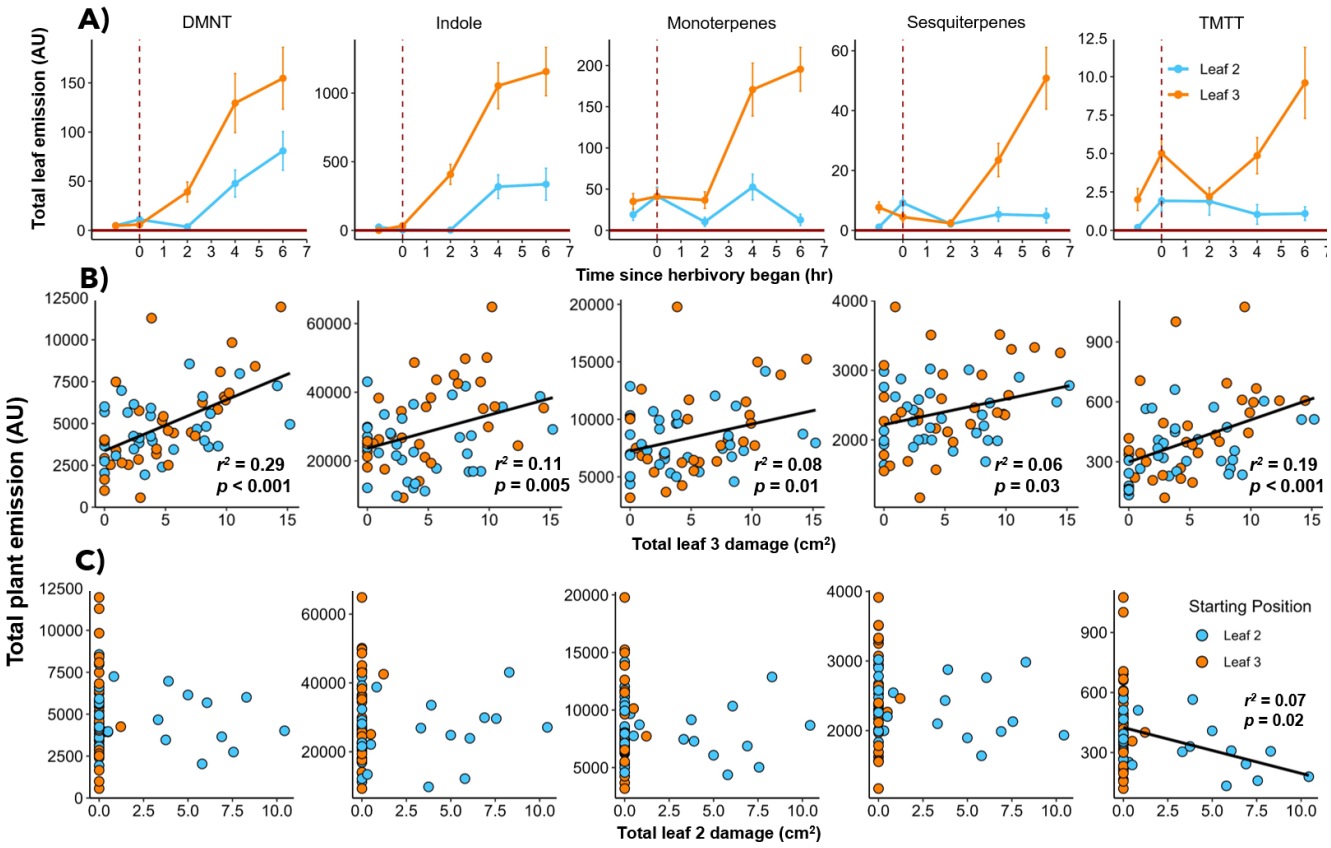

Figure 6. Leaf 3 plays a determinant role in overall herbivore-induced volatile emission during *Spodoptera exigua* herbivory. A) Emission from *S. exigua*-fed detached leaves from V2-stage seedlings. B) Correlation of total plant-level emission with total leaf 3 damage after 6 hr of herbivory. C) Correlation of total volatile emission with total leaf 2 damage after 6 hr of herbivory. B and C depict the same individual plants. Colored points represent biological replicates and black lines represent significant linear relationships between emission and damage.

371

372 In addition to monitoring how herbivores mediate volatile emission patterns, we aimed to

373 investigate how maize leaves differentially impact herbivore performance. Both *S. exigua* and

374 *S. littoralis* damaged leaf 3 to a greater extent than leaf 2 in detached leaves (Fig 7A). After

375 48 hr of feeding, there were no clear differences in relative growth rate for either species

376 between leaf 2- and leaf 3-fed larvae (Fig 7C).

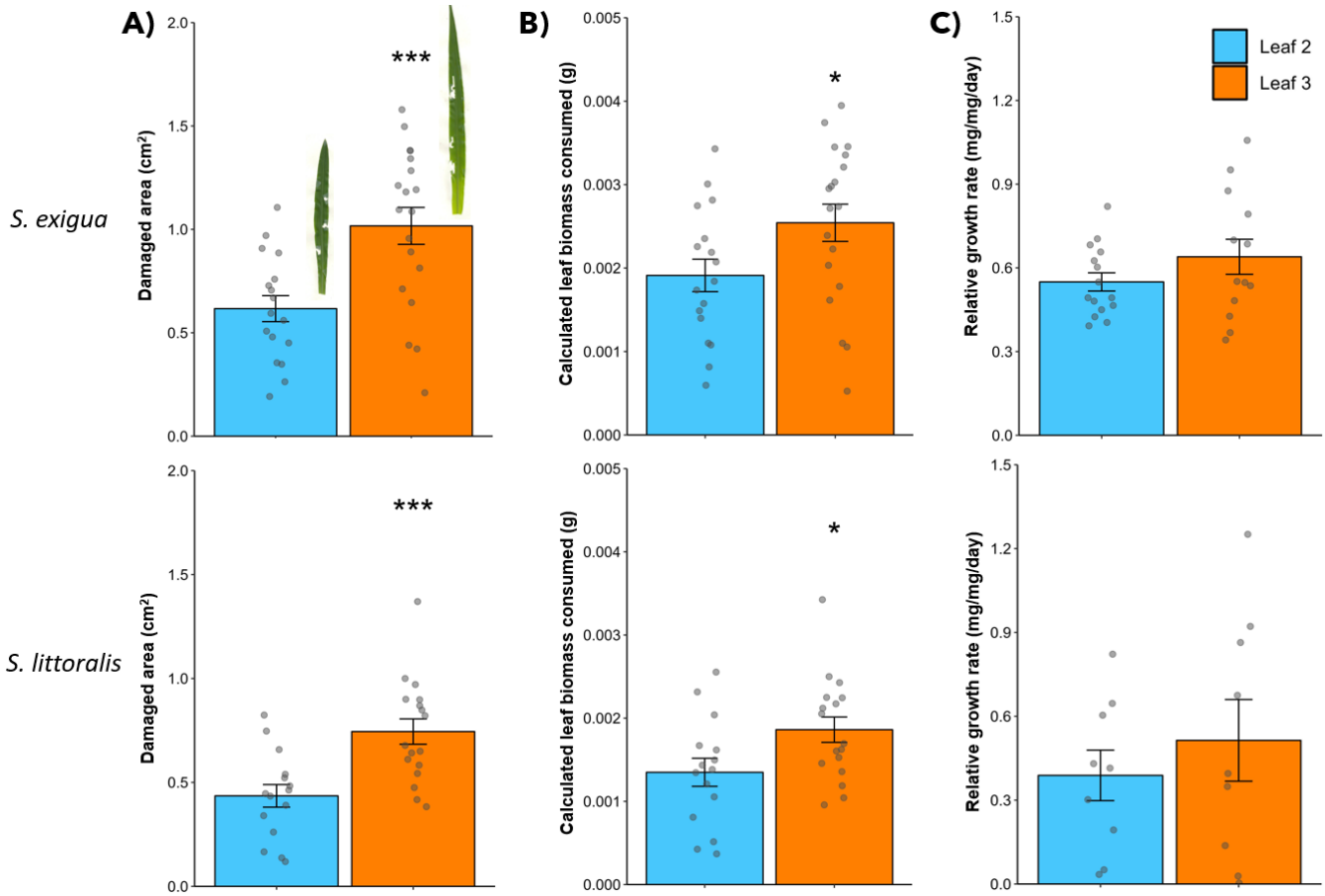

Figure 7. Generalist herbivores damage a greater area of leaf 3 with no performance benefit. A) Area of leaf tissue consumed by 4th instar *Spodoptera exigua* and *S. littoralis* after 6 hr feeding on detached leaves from V2-stage seedlings, B) calculated biomass consumption based on leaf mass per area (LMA) of leaf 2 (0.0031) and leaf 3 (0.0025), and C) relative growth rate of 4th *S. exigua* and *S. littoralis* after 48 hr of feeding. * = $p < 0.05$, *** = $p < 0.001$ as determined by Welch's two-sample *t*-test. Grey points represent biological replicates. Bars = mean ± SE. For *S. exigua* n = 13-19, for *S. littoralis* n = 9-17.

Discussion

Spatiotemporal and developmental patterns have been shown influence volatile emissions in ecologically important ways (Köllner *et al.*, 2013; Wang *et al.*, 2023; Waterman *et al.*, 2024). We show that size of the damaged maize leaves plays a determinant role in the overall plant-level volatile emissions and that generalist herbivores preferentially feed on the leaves that result in the highest volatile emissions. Here we discuss the mechanisms and potential implications of these patterns.

Within-plant spatiotemporal patterns are known to be important factors mediating stress responses (Barton *et al.*, 2010; Köhler *et al.*, 2015; Wang *et al.*, 2023). Given maize seedlings differentially emit volatiles depending on the location of damage, one possible explanation for this variability could be differing induction capacities or systemic signaling capabilities between foliar tissues (Köllner *et al.*, 2013; Irmisch *et al.*, 2014). However, our data show minimal differences in induction between leaves; volatile biosynthesis genes are not only comparable across locally-damaged leaves, but the capacity for induction in undamaged, systemic leaves are consistent regardless of where damage occurs. A similar pattern was found for HDMBOA-Glc, which is a compound known to play an important role in direct defense against chewing herbivores such as *Spodoptera* spp. (Glauser *et al.*, 2011; Tzin *et al.*, 2017; Li *et al.*, 2018). As such, per unit tissue, induction capacity is similar between V2-stage maize seedling leaves, most clearly shown between leaf 2 and leaf 3. Nevertheless, it is possible that underdeveloped defense machinery and gas exchange capacity in the emerging leaf 4 contributes to the apparent reductions in volatile emissions in leaf 4 (Wang *et al.*, 2019; Wang *et al.*, 2023). Based on these findings, it is clear that differences in emission based on damage location is not driven by differences in defense inducibility between leaves.

Leaf size seems to be the determinant factor controlling volatile emissions in maize seedlings, as there are very strong and consistent relationships between emission and both damaged-leaf mass and area across developmental stages. While there is generally a strong relationship between emission and area, it is not as robust as the relationship between emission and biomass. As such, it is likely that emission is a function of both area, whereby greater area equates to more points of exit for volatiles (e.g., more stomata), and thickness, whereby

thicker leaves may have more tissue capable of producing these volatiles. Biomass is a function of both area and thickness, which likely explains why this relationship is strongest.

The relationship between emission and leaf size is also clearly strongest for leaves that are actively developing. As developing leaves show greater variation in mass and area than fully-developed leaves (Powell & Lenhard, 2012), the close relationship between size and emission is apparent. Once leaves are fully developed there is much lower variation in size between leaves, however there are still differences in emission between individual leaves. We have previously identified leaf development as a factor that influences volatile emissions (Wang *et al.*, 2023), and our findings in the present study support this; when immature and mature leaves are comparable in size, mature leaves emit more volatiles given equal damage.

While green leaf volatiles are formed in, and emitted directly from, wounded tissues (Hatanaka, 1993; Matsui *et al.*, 2000; Escobar-Bravo *et al.*, 2023), other volatiles such as terpenes and indole are produced *de novo* and systemically over time following stress (Erb *et al.*, 2015), and emissions of these compounds are likely regulated by stomatal aperture (Niinemets, 2003; Seidl-Adams *et al.*, 2015; Maleki *et al.*, 2024). Some herbivores have been shown to excrete enzymes, such as glucose oxidase, which close stomata and minimize volatile emissions during feeding (Lin *et al.*, 2021). Nevertheless, the relationship between herbivore feeding behavior and volatile emissions is not well understood. We find that two generalist herbivores preferentially feed on the leaves that result in the highest local and plant-level volatile emissions. As herbivores feed more heavily on leaf 3, which emits the most volatiles, we reasoned that there would be a clear benefit for herbivores to eat this leaf. However, surprisingly, this was not the case. In fact, what we observed was that, in order to

434 reach the same level of growth, herbivores must consume more leaf 3 tissue compared to leaf
435 2, resulting in even greater volatile emissions. Even in intact plants, where herbivores can
436 move freely over the entire plant, herbivores chose to consume leaf 3 most, which has a
437 determinant impact on overall volatile emissions in maize seedlings. As a result, *Spodoptera*
438 larvae may reveal themselves to the environment by feeding on the tissues that release the
439 most volatiles. Herbivore-induced volatile emissions can be disadvantageous for herbivores
440 through direct toxicity (Veyrat *et al.*, 2016; Chen *et al.*, 2021; Chen *et al.*, 2023), enhanced
441 attraction of natural enemies (Michereff *et al.*, 2019), oviposition deterrence (Signoretti *et al.*,
442 2012), and population and community resistance by enhancing neighboring plant defenses
443 (Escobar-Bravo *et al.*, 2023; Waterman *et al.*, 2024). On the other hand, they can also be
444 advantageous by confusing natural enemies and can be used by herbivores for host location
445 (Poelman *et al.*, 2012; Zu *et al.*, 2020). Additionally, it has been shown that relative ratios and
446 blends of emitted compounds, beyond absolute amounts can shape volatile-mediated
447 interactions between plants and the environment (Allmann & Baldwin, 2010; Fouchier *et al.*,
448 2018). More research is required to understand to the consequences of increased volatile
449 emissions in the atmosphere, as well as the potential fitness costs and benefits of herbivore
450 feeding behavior in this context.

451

452 In conclusion, our work shows that the size of damaged leaves determines the extent of
453 damage-induce volatiles emitted from maize seedlings. While tissue damage can be inflicted
454 by many abiotic and biotic stressors, it is particularly noteworthy that, in addition to
455 mechanical damage, patterns are consistent with real herbivore feeding. Our work provides a
456 basis for developing a deeper understanding of the precise nature of herbivore feeding
457 patterns and defense phenotypes, and how the interaction of the two can yield potentially
458 important ecological outcomes for both plants and herbivores.

459

460 ## Supplemental Tables

Supplemental Table 1. Gene identifiers and qRT-PCR primer sequences used in this study.

Target gene	Gene name	Identifier	fw	rv
TPS2	Terpene synthase 2	Zm00001d015053	TACCGGGTCGAGATCACCAA	TCGTTCGTAACGGTGTGGAG
TPS10	Terpene synthase 10	Zm00001d024486	TGACAGCCTTGATCACCGTA	AGTTCATCCCCACACGAATC
CYP92C5	Dimethylnonatriene/ trimethyltridecatetraene synthase	Zm00001d018839	AGGGGTTCAAGCGGAAGATG	AGGTCAGTCGCCACAAACTC
IGL	Indole-3-glycerol phosphate lyase	Zm00001d034453	GAGCTGGTGCTGCTCACA	GCGCGTGGACCTGTAACT
UBI1	Ubiquitin	Zm00001d015327	TAAGCTGCCGATGTGCCTGCG	CTGAAAGACAGAACATAATGAGCACAG

461

462

Supplemental Table 2. ANOVA and Kruskal-Wallis test results from data presented in the main text. Bold values: $p < 0.05$. Abbreviations: TPS2 = terpene synthase 2, TPS10 = terpene synthase 10, CYP92C5 = Dimethylnonatriene/trimethyltetradecatetraene synthase, IGL = indole-3-glycerol phosphate lyase, DMNT = 4,8-dimethylnona-1,3,7-triene, MNT = monoterpenes, SQT = sesquiterpenes, TMTT = 4,8,12-trimethyltrideca-1,3,7,11-tetraene, *S.e* = *Spodoptera exigua*, *S.l* = *Spodoptera littoralis*

	Damage location			**Leaf**			**Dam x Leaf**		
	F	*p*	*df*	F/χ^2	*p*	*df*	*F*	*p*	*df*
Gene expression (Fig 2)									
TPS2	135.68	**< 0.001**	3	10.65	**< 0.001**	2	11.49	**< 0.001**	6
TPS10	454.67	**< 0.001**	3	0.88	0.42	2	16.16	**< 0.001**	6
CYP92C5	87.16	**< 0.001**	3	1.74	0.19	2	1.73	0.13	6
IGL	82.82	**< 0.001**	3	6.64	**0.003**	2	2.55	**0.03**	6
Leaf mass (Fig 4A-B)									
Entire leaves	-	-	-	119.72	**< 0.001**	2	-	-	-
Cut leaves	-	-	-	1.53	0.25	2	-	-	-
Plant damage (Fig 5)									
S.e leaf 2	-	-	-	44.01	**< 0.001**	3	-	-	-
S.e leaf 3	-	-	-	89.39	**< 0.001**	3	-	-	-
S.l leaf 2	-	-	-	8.31	**0.04**	3	-	-	-
S.l leaf 3	-	-	-	36.86	**< 0.001**	3	-	-	-

463

Supplemental Table 3. Welch's two-sample t-test results for herbivore performance parameters between detached leaf 2 and leaf 3

Response	*Spodoptera exigua*			*Spodoptera littoralis*		
	t	*p*	df	t	*p*	df
Damage	-3.67	**<0.001**	31	-3.79	**<0.001**	29
Mass con.	-2.13	**0.04**	33	-2.26	**0.03**	29
RGR	-1.27	0.22	18	-0.73	0.48	13

464

465

466 ## References

467 **Allmann S, Baldwin IT. 2010.** Insects Betray Themselves in Nature to Predators by Rapid
468 Isomerization of Green Leaf Volatiles. *Science* **329**: 1075–1078.
469 **Barton KE, Koricheva J, Associate Editor: Tia-Lynn Ashman, Editor: Donald L. DeAngelis. 2010.** The
470 Ontogeny of Plant Defense and Herbivory: Characterizing General Patterns Using Meta-Analysis.
471 *The American Naturalist* **175**: 481–493.
472 **Bellec L, Seimandi-Corda G, Menacer K, Trabalon M, Ollivier J, Lunel C, Faure S, Cortesero A-M,**
473 **Hervé M. 2022.** Factors driving the within-plant patterns of resource exploitation in a herbivore.
474 *Functional Ecology* **36**: 1700–1712.
475 **Block AK, Vaughan MM, Schmelz EA, Christensen SA. 2019.** Biosynthesis and function of terpenoid
476 defense compounds in maize (*Zea mays*). *Planta* **249**: 21–30.
477 **Bustos-Segura C, González-Salas R, Benrey B. 2022.** Early damage enhances compensatory
478 responses to herbivory in wild lima bean. *Frontiers in Plant Science* **13**.
479 **Chen C, Chen H, Huang S, Jiang T, Wang C, Tao Z, He C, Tang Q, Li P. 2021.** Volatile DMNT directly
480 protects plants against *Plutella xylostella* by disrupting the peritrophic matrix barrier in insect
481 midgut. *eLife* **10**.
482 **Chen H, Chen C, Huang S, Zhao M, Wang T, Jiang T, Wang C, Tao Z, Zhang Y, Wang Y *et al.* 2023.**
483 Inactivation of RPX1 in Arabidopsis confers resistance to Plutella xylostella through the
484 accumulation of the homoterpene DMNT. *Plant, Cell & Environment* **46**: 946–961.
485 **Eisenring M, Meissle M, Hagenbucher S, Naranjo SE, Wettstein F, Romeis J. 2017.** Cotton Defense
486 Induction Patterns Under Spatially, Temporally and Quantitatively Varying Herbivory Levels.
487 *Frontiers in Plant Science* **8**.
488 **Erb M, VEYRAT N, Robert CAM, Xu H, Frey M, Ton J, Turlings TCJ. 2015.** Indole is an essential
489 herbivore-induced volatile priming signal in maize. *Nat. Commun.* **6**: 6273.
490 **Escobar-Bravo R, Lin P-A, Waterman JM, Erb M. 2023.** Dynamic environmental interactions shaped
491 by vegetative plant volatiles. *Nat. Prod. Rep.* doi: 10.1039/D2NP00061J.
492 **Fouchier A** de, **Sun X, Caballero-Vidal G, Travaillard S, Jacquin-Joly E, Montagné N. 2018.** Behavioral
493 Effect of Plant Volatiles Binding to Spodoptera littoralis Larval Odorant Receptors. *Front. Behav.*
494 *Neurosci.* **12**.

Frey M, Stettner C, Paré PW, Schmelz EA, Tumlinson JH, Gierl A. 2000. An herbivore elicitor activates the gene for indole emission in maize. *Proceedings of the National Academy of Sciences* **97**: 14801–14806.

Glauser G, Marti G, Villard N, Doyen GA, Wolfender J-L, Turlings TC, Erb M. 2011. Induction and detoxification of maize 1,4-benzoxazin-3-ones by insect herbivores. *The Plant Journal* **68**: 901–911.

Gonin M, Lopez-Hilfiker F, Hutterli M, Erb M, Pflander M. 2018. AUTOSAMPLER.

Groen SC, Jiang S, Murphy AM, Cunniffe NJ, Westwood JH, Davey MP, Bruce TJA, Caulfield JC, Furzer OJ, Reed A *et al.* 2016. Virus Infection of Plants Alters Pollinator Preference: A Payback for Susceptible Hosts? *PLOS Pathogens* **12**: e1005790.

Hajdu C, Molnár BP, Waterman JM, Machado RAR, Radványi D, Fónagy A, Khan SA, Vassor T, Biet B, Erb M *et al.* 2024. Volatile-mediated oviposition preference for healthy over root-infested plants by the European corn borer. *Plant, Cell & Environment* **n/a**.

Hatanaka A. 1993. The biogeneration of green odour by green leaves. *Phytochemistry* **34**: 1201–1218.

Heil M, Silva Bueno JC. 2007. Within-plant signaling by volatiles leads to induction and priming of an indirect plant defense in nature. *Proceedings of the National Academy of Sciences* **104**: 5467–5472.

Hunziker P, Lambertz SK, Weber K, Crocoll C, Halkier BA, Schulz A. 2021. Herbivore feeding preference corroborates optimal defense theory for specialized metabolites within plants. *Proceedings of the National Academy of Sciences* **118**: e2111977118.

Irmisch S, Jiang Y, Chen F, Gershenzon J, Köllner TG. 2014. Terpene synthases and their contribution to herbivore-induced volatile emission in western balsam poplar (Populus trichocarpa). *BMC Plant Biology* **14**: 270.

KATTGE J, DÍAZ S, LAVOREL S, PRENTICE IC, Leadly P, BÖNISCH G, Garnier E., WESTOBY M, REICH PB, WRIGHT IJ *et al.* 2011. TRY – a global database of plant traits. *Global Change Biology* **17**: 2905–2935.

Köhler A, Maag D, VEYRAT N, Glauser G, Wolfender J-L, TURLINGS TCJ, Erb M. 2015. Within-plant distribution of 1,4-benzoxazin-3-ones contributes to herbivore niche differentiation in maize. *Plant, Cell & Environment* **38**: 1081–1093.

Köllner TG, Lenk C, Schnee C, Köpke S, Lindemann P, Gershenzon J, Degenhardt J. 2013. Localization of sesquiterpene formation and emission in maize leaves after herbivore damage. *BMC Plant Biology* **13**: 15.

Li B, Förster C, Robert CAM, Züst T, Hu L, Machado RAR, Berset J-D, Handrick V, Knauer T, Hensel G *et al.* 2018. Convergent evolution of a metabolic switch between aphid and caterpillar resistance in cereals. *Science Advances* **4**: eaat6797.

Liao P, Ray S, Boachon B, Lynch JH, Deshpande A, McAdam S, Morgan JA, Dudareva N. 2021. Cuticle thickness affects dynamics of volatile emission from petunia flowers. *Nature Chemical Biology* **17**: 138–145.

Lin P-A, Chen Y, Chaverra-Rodriguez D, Heu CC, Zainuddin NB, Sidhu JS, Peiffer M, Tan C-W, Helms A, Kim D *et al.* 2021. Silencing the alarm: an insect salivary enzyme closes plant stomata and inhibits volatile release. *New Phytologist* **230**: 793–803.

Lin P-A, Chen Y, Ponce G, Acevedo FE, Lynch JP, Anderson CT, Ali JG, Felton GW. 2022. Stomata-mediated interactions between plants, herbivores, and the environment. *Trends in Plant Science* **27**: 287–300.

Maag D, Dalvit C, Thevenet D, Köhler A, Wouters FC, Vassão DG, Gershenzon J, Wolfender J-L, Turlings TCJ, Erb M *et al.* 2014. 3-β-D-Glucopyranosyl-6-methoxy-2-benzoxazolinone (MBOA-N-Glc) is an insect detoxification product of maize 1,4-benzoxazin-3-ones. *Phytochem.* **102**: 97–105.

Maag D, Erb M, Bernal JS, Wolfender J-L, Turlings TCJ, Glauser G. 2015. Maize Domestication and Anti-Herbivore Defences: Leaf-Specific Dynamics during Early Ontogeny of Maize and Its Wild Ancestors. *PloS one* **10**: e0135722.

Maag D, Köhler A, Robert CA, Frey M, Wolfender J-L, Turlings TC, Glauser G, Erb M. 2016. Highly localized and persistent induction of Bx1-dependent herbivore resistance factors in maize. *The Plant Journal* **88**: 976–991.

Maleki FA, Seidl-Adams I, Felton GW, Kersch-Becker MF, Tumlinson JH. 2024. Stomata: gatekeepers of uptake and defense signaling by green leaf volatiles in maize. *Journal of Experimental Botany*: erae401.

Matsui K. 2006. Green leaf volatiles: hydroperoxide lyase pathway of oxylipin metabolism. *Current Opinion in Plant Biology* **9**: 274–280.

Matsui K, Kurishita S, Hisamitsu A, Kajiwara T. 2000. A lipid-hydrolysing activity involved in hexenal formation. *Biochemical Society Transactions* **28**: 857–860.

Maurya AK, Patel RC, Frost CJ. 2020. Acute toxicity of the plant volatile indole depends on herbivore specialization. *Journal of Pest Science* **93**: 1107–1117.

Michereff MFF, Magalhães DM, Hassemer MJ, Laumann RA, Zhou J-J, Ribeiro, Paulo E. de A., Viana PA, Guimarães, Paulo E. de O., Schimmelpfeng PHC, Borges M *et al.* 2019. Variability in herbivore-induced defence signaling across different maize genotypes impacts significantly on natural enemy foraging behaviour. *Journal of Pest Science* **92**: 723–736.

Mithöfer A, Wanner G, Boland W. 2005. Effects of feeding *Spodoptera littoralis* on lima bean leaves. II. Continuous mechanical wounding resembling insect feeding is sufficient to elicit herbivory-related volatile emission. *Plant Physiol.* **137**: 1160–1168.

Niinemets Ü. 2003. Controls on the emission of plant volatiles through stomata: A sensitivity analysis. *J. Geophys. Res.* **108**.

Ohnmeiss TE, Baldwin IT. 2000. OPTIMAL DEFENSE THEORY PREDICTS THE ONTOGENY OF AN INDUCED NICOTINE DEFENSE. *Ecology* **81**: 1765–1783.

Orrock JL, Guiden PW, Pan VS, Karban R. 2022. Plant induced defenses that promote cannibalism reduce herbivory as effectively as highly pathogenic herbivore pathogens. *Oecologia* **199**: 397–405.

Pan VS, Wetzel WC. 2024. Neutrality in plant–herbivore interactions. *Proceedings of the Royal Society B: Biological Sciences* **291**: 20232687.

Poelman EH, Bruinsma M, Zhu F, Weldegergis BT, Boursault AE, Jongema Y, van Loon JJA, Vet LEM, Harvey JA, Dicke M. 2012. Hyperparasitoids Use Herbivore-Induced Plant Volatiles to Locate Their Parasitoid Host. *PLOS Biology* **10**: e1001435.

Powell AE, Lenhard M. 2012. Control of Organ Size in Plants. *Current Biology* **22**: R360-R367.

R Core Team. 2022. R: A language and environment for statistical computing. Vienna, Austria: R Foundation for Statistical Computing.

Raissig MT, Matos JL, Anleu Gil MX, Kornfeld A, Bettadapur A, Abrash E, Allison HR, Badgley G, Vogel JP, Berry JA *et al.* 2017. Mobile MUTE specifies subsidiary cells to build physiologically improved grass stomata. *Science* **355**: 1215–1218.

Richter A, Schaff C, Zhang Z, Lipka AE, Tian F, Köllner TG, Schnee C, Preiß S, Irmisch S, Jander G *et al.* 2016. Characterization of Biosynthetic Pathways for the Production of the Volatile Homoterpenes DMNT and TMTT in *Zea mays*. *Plant Cell* **28**: 2651–2665.

Schnee C, Köllner TG, Held M, Turlings TCJ, Gershenzon J, Degenhardt J. 2006. The products of a single maize sesquiterpene synthase form a volatile defense signal that attracts natural enemies of maize herbivores. *Proceedings of the National Academy of Sciences* **103**: 1129–1134.

Seidl-Adams I, Richter A, Boomer KB, Yoshinaga N, Degenhardt J, Tumlinson JH. 2015. Emission of herbivore elicitor-induced sesquiterpenes is regulated by stomatal aperture in maize (*Zea mays*) seedlings. *Plant Cell Environ.* **38**: 23–34.

Signoretti AGC, Peñaflor, M. F. G. V., Bento JMS. 2012. Fall Armyworm, Spodoptera frugiperda (J.E. Smith) (Lepidoptera: Noctuidae), Female Moths Respond to Herbivore-Induced Corn Volatiles. *Neotropical Entomology* **41**: 22–26.

The Herbivory Variability Network* †, Robinson ML, Hahn PG, Inouye BD, Underwood N, Whitehead SR, Abbott KC, Bruna EM, Cacho NI, Dyer LA *et al.* 2023. Plant size, latitude, and phylogeny explain within-population variability in herbivory. *Science* **382**: 679–683.

Turlings TC, Erb M. 2018. Tritrophic Interactions Mediated by Herbivore-Induced Plant Volatiles: Mechanisms, Ecological Relevance, and Application Potential. *Annual Review of Entomology* **63**: 433–452.

Tzin V, Hojo Y, Strickler SR, Bartsch LJ, Archer CM, Ahern KR, Zhou S, Christensen SA, Galis I, Mueller LA *et al.* 2017. Rapid defense responses in maize leaves induced by Spodoptera exigua caterpillar feeding. *Journal of Experimental Botany* **68**: 4709–4723.

van den Berg J, Britz C, Du Plessis H. 2021. Maize Yield Response to Chemical Control of Spodoptera frugiperda at Different Plant Growth Stages in South Africa. *Agriculture* **11**.

Veyrat N, Robert CAM, Turlings TCJ, Erb M. 2016. Herbivore intoxication as a potential primary function of an inducible volatile plant signal. *Journal of Ecology* **104**: 591–600.

Wang H, Guo S, Qiao X, Guo J, Li Z, Zhou Y, Bai S, Gao Z, Wang D, Wang P *et al.* 2019. BZU2/ZmMUTE controls symmetrical division of guard mother cell and specifies neighbor cell fate in maize. *PLOS Genetics* **15**: e1008377.

Wang L, Jäggi S, Cofer TM, Waterman JM, Walthert M, Glauser G, Erb M. 2023. Immature leaves are the dominant volatile-sensing organs of maize. *Curr. Biol.* **33**: 3679-3689.e3.

Waterman JM, Cazzonelli CI, Hartley SE, Johnson SN. 2019. Simulated Herbivory: The Key to Disentangling Plant Defence Responses. *Trends Ecol. Evol.* **34**: 447–458.

Waterman JM, Cibils-Stewart X, Cazzonelli CI, Hartley SE, Johnson SN. 2021. Short-term exposure to silicon rapidly enhances plant resistance to herbivory. *Ecology* **102**: e03438.

Waterman JM, Cofer TM, Wang L, Glauser G, Erb M, Rasmann S, Weigel D. 2024. High-resolution kinetics of herbivore-induced plant volatile transfer reveal clocked response patterns in neighboring plants. *eLife* **12**: RP89855.

White H. 1980. A Heteroskedasticity-Consistent Covariance Matrix Estimator and a Direct Test for Heteroskedasticity. *Econometrica* **48**: 817–838.

Zu P, Boege K, Del-Val E, Schuman MC, Stevenson PC, Zaldivar-Riverón A, Saavedra S. 2020. Information arms race explains plant-herbivore chemical communication in ecological communities. *Science* **368**: 1377–1381.